Available online at www.sciencedirect.com
SCIENCE DIRECT®

Journal of the European Ceramic Society 23 (2003) 1345–1353
www.elsevier.com/locate/jeurceramsoc

Electrical properties and stability of praseodymium oxide-based ZnO varistor ceramics doped with Er_2O_3

Choon-Woo Nahm

Department of Electrical Engineering, Dongeui University, Busan 614-714, South Korea

Received 29 March 2002; received in revised form 16 July 2002; accepted 7 August 2002

Abstract

The electrical properties and its stability against DC accelerated aging stress of Pr_6O_{11}-based ZnO varistor ceramics were investigated with Er_2O_3 content and sintering time. The nonlinear exponent of varistors with increasing Er_2O_3 content varied with V-shape, reaching minimum at 1.0 mol% Er_2O_3. As sintering time is increased, the nonlinear exponent was decreased, whereas its stability for DC stress was improved. The varistor with 0.5 mol% Er_2O_3 sintered at 1340 °C for 2 h exhibited the best performance for the nonlinearity and stability. This varistor exhibited not only high nonlinearity, with the nonlinear exponent of 43.4 and the leakage current of 1.2 μA, but also high stability, with the variation rates of varistor voltage and nonlinear exponent is −1.5 and −2.5%, respectively, under DC stress, such as $(0.80V_{1\ mA}/90\ °C/12\ h)+(0.85V_{1\ mA}/115\ °C/\ 12\ h)+(0.90V_{1\ mA}/120\ °C/12\ h)+(0.95V_{1\ mA}/125\ °C/12\ h)+(0.95V_{1\ mA}/150\ °C/12\ h)$.

Keywords: Aging; Electrical properties; Grain boundaries; Varistors; ZnO

1. Introduction

ZnO varistors are multi-junction ceramic semiconductor devices made by sintering ZnO powder with other metal oxides of small amount, in addition to varistor-forming oxides such as Bi_2O_3, Pr_6O_{11}, V_2O_5, and BaO. Sintering process gives rise to a structure, which consists of semiconducting *n*-type ZnO grains surrounded by very thin insulating intergranular layers.[1] A unit structure consisted of ZnO grain-intergranular layer-ZnO grain structure distributes as three-dimensional series-parallel network to an entire ceramic bulk. A unit structure corresponds to a micro-varistor with a single junction. ZnO varistors exhibit highly nonlinear voltage–current (*V–I*) properties expressed by the relation $I=KV^{\alpha}$, where *K* is a constant and α is a nonlinear exponent, which characterizes the nonlinear properties of varistors. They act as an insulator below the varistor voltage, called the breakdown voltage, and conductor thereafter. The nonlinear *V–I* characteristics of ZnO varistors are generated by many double Schottky barriers at the grain boundary layers, which are essentially formed through the segregation of varistor-forming oxide. Moreover, they possess excellent surge-withstanding capability. Therefore, they have been extensively used as a core element of surge absorbers in electronic circuits and of surge arresters in electric power systems.[2]

At present, the majority of commercially available ZnO varistors is Bi_2O_3-based ZnO varistors showing excellent varistor properties, but they have a few flaws due to Bi_2O_3 having a high volatility and reactivity.[3] The former changes varistor characteristics with the variation of inter-composition ratio of additives, the latter destroys the multilayer structure of chip varistors, and it generates an additional insulating spinel phase, which does not play any role in electrical conduction. And another flaw is Bi_2O_3-based varistors need many additives to obtain high nonlinearity and stable electrical properties.

To overcome the problems in Bi_2O_3-based varistors, as mentioned just above, Pr_6O_{11}-based ZnO varistors doped with praseodymium oxides (Pr_6O_{11}) as a varistor-forming oxide have been reported.[4–15] The features of these varistors are that they indicated not only simple

E-mail address: cwnahm@dongeui.ac.kr (C.-W. Nahm).

0955-2219/03/$ - see front matter © 2002 Elsevier Science Ltd. All rights reserved.
PII: S0955-2219(02)00285-6

microstructure consisting of ZnO grain and intergranular layer, unlike the Bi_2O_3-doped varistors, but also high nonlinearity, with a nonlinear exponent of 25–37 only for ternary system ZnO–Pr_6O_{11}–CoO, compared with Bi_2O_3-based ZnO varistors having a nonlinear exponent of 13–18 for only ternary system ZnO-Bi_2O_3–CoO (or MnO). However, most of Pr_6O_{11}-based ZnO varistors studied were limited to ternary system ZnO–Pr_6O_{11}–CoO and further, the stability of *V–I* characteristics for ternary system has not been reported. To apply Pr_6O_{11}-based varistors in various areas, the effect of the variables, such as the kind and amount of additives, composition ratio, and sintering process on the electrical properties and stability of Pr_6O_{11}-based varistors should be continuously and diversely studied. Many researchers who are interested in varistors wish to fabricate ZnO varistors exhibiting densified microstructure, high nonlinearity, and high stability.

Recently, Nahm et al. reported that the addition of rare-earth oxides (Er_2O_3, Dy_2O_3) to ZnO–Pr_6O_{11}–CoO based varistors improves the nonlinearity and electrical stability.[7–15] However, the varistors having a high stability never exceeded 40 in the nonlinear exponent and the varistors having a high nonlinearity exhibited very poor stability for DC stress. Further, the varistors added by Cr_2O_3 to quaternary system above exhibited excellent nonlinear exponent close to 70 and the stability for any varistor is greatly improved.[14]

The purpose of this work is to investigate electrical characteristics and its stability for DC accelerated aging stress according to Er_2O_3 content and sintering time in ZnO–Pr_6O_{11}–CoO–Cr_2O_3-Er_2O_3-based (ZPCCE) varistors and to discuss a correlation between densification of ceramics and electrical stability for DC accelerated aging stress.

2. Experimental procedure

Reagent-grade raw materials with composition ratio of (98-x) mol% ZnO, 0.5 mol% Pr_6O_{11}, 1.0 mol% CoO, 0.5 mol% Cr_2O_3, ($x = 0.5$–2.0) mol% Er_2O_3 were used as the starting materials for ZPCCE varistors. Raw materials were mixed by ball milling with zirconia balls and acetone in a polypropylene bottle for 24 h. The mixture was dried at 120 °C for 12 h and calcined in air at 750 °C for 2 h. The calcined mixture was pulverized using an agate mortar/pestle and after 2 wt.% polyvinyl alcohol (PVA) binder addition, granulated by sieving 200-mesh screen to produce starting powder. The powder was uniaxially pressed into discs of 10 mm in diameter and 2 mm in thickness at a pressure of 800 kg/cm^2. The discs were covered with raw powder in alumina crucible, sintered at 1340 °C in air for 1–2 h, and furnace-cooled to room temperature. The heating and cooling rates were 4 °C/min. The sintered samples were lapped and polished to 1.0 mm thickness. The size of the final samples was about 8 mm in diameter and 1.0 mm in thickness. Silver paste was coated on both faces of the samples and the ohmic contact of electrodes was formed by heating at 600 °C for 10 min. The size of electrodes was 5 mm in diameter.

The voltage–current (*V–I*) characteristics of ZPCCE varistors were measured by stepping up the linear stair voltage in increment of 0.5 V using a programmable Keithley 237 unit. To avoid joule heat of varistors, the varistors were applied up to 50 mA/cm^2. The varistor voltage ($V_{1\ mA}$) was measured at 1.0 mA/cm^2 and the leakage current (I_l) was defined as the current at 0.80 $V_{1\ mA}$. In addition, the nonlinear exponent (α) is defined from $\alpha = 1/(\log E_2 - \log E_1)$, where E_1 and E_2 are the electric fields corresponding to 1.0 mA/cm^2 and 10 mA/cm^2, respectively.

The capacitance–voltage (*C–V*) characteristics of ZPCCE varistors were measured at 1 kHz with the variable applied bias in the pre-breakdown region of the *V–I* characteristics using a QuadTech 7600 RLC meter and a Keithley 617 electrometer. The donor concentration (N_d) of ZnO grains and the barrier height (ϕ_b) at the grain boundary were determined from the slope and intercept of straight line, respectively, using the equation $(1/C_b - 1/2C_{bo})^2 = 2(\phi_b + V_{gb})/q\varepsilon\ N_d$ proposed by Mukae et al.,[16] where C_b is the capacitance per unit area of a grain boundary, C_{bo} is the value of C_b when $V_{gb} = 0$, V_{gb} is the applied voltage per grain boundary, q is the electronic charge, ε is the permittivity of ZnO ($\varepsilon = 8.5\varepsilon_o$). The density of interface states (N_t) at the grain boundary was determined by the equation $N_t = (2\varepsilon N_d \phi_b/q)^{1/2}$ using the value of the donor concentration and barrier height obtained above.[16] Once the donor concentration and barrier height are known, the depletion layer width (t) of the either side at the grain boundaries was determined by the equation $N_d\ t = N_t$.[17]

The stability tests for DC accelerated aging stress were performed under five continuous conditions, such as 0.80 $V_{1\ mA}$/ 90 °C/12 h in the first stress, 0.85 $V_{1\ mA}$/ 115 °C/12 h in the second stress, 0.90 $V_{1\ mA}$/120 °C/12 h in the third stress, 0.95 $V_{1\ mA}$/125 °C/12 h in the fourth stress, and 0.95 $V_{1\ mA}$/150 °C/12 h in the fifth stress. Simultaneously, the leakage current during the stress time was monitored at intervals of 1 min by a Keithley 237 unit.

The either surface of samples, after the electrical measurement has finished, was lapped and ground with SiC paper and polished with 0.3 μm-Al_2O_3 powder to a mirror-like surface. The polished samples were thermally etched at 1100 °C for 30 min. The surface of samples was metallized with a thin coating of Au to reduce charging effects and to improve the resolution of the image. The surface microstructure was examined by a scanning electron microscope (SEM, Hitachi S2400,

Japan). The average grain size (d) was determined by the lineal intercept method, given by $d = 1.56L/MN$, where L is the random line length on the micrograph, M is the magnification of the micrograph, and N is the number of the grain boundaries intercepted by lines.[18] The density (ρ) of ZPCCE ceramics was measured by the Archimedes method.

3. Results and discussion

Fig. 1 shows SEM micrographs of ZPCCE ceramics sintered for 1–2 h with Er_2O_3 content. It was identified by XRD, which does not exhibit here, that the phases of ZPCCE ceramics are not different from those of ZPCE ($ZnO–Pr_6O_{11}–CoO–Er_2O_3$) ceramics with no Cr_2O_3, which consist of ZnO grains and Er- and Pr-rich intergranular layers.[12] Er oxide and Pr oxide were found to coexist in the grain boundaries and the nodal points as if they were a single phase. It was observed by SEM that as Er_2O_3 content is increased, the intergranular phase such as Er- and Pr-rich phase was gradually more distributed at the grain boundaries and the nodal points particularly. The detailed microstructural parameters, including the average grain size (d), density (ρ), shrinkage (S), and porosity (P) are summarized in Table 1. The average grain size of ceramics was decreased in the range of 9.7–5.1 μm for sintering time of 1 h and 12.1–6.8 μm for 2 h with increasing Er_2O_3 content. Therefore, Er_2O_3 serves as inhibitor for grain growth.

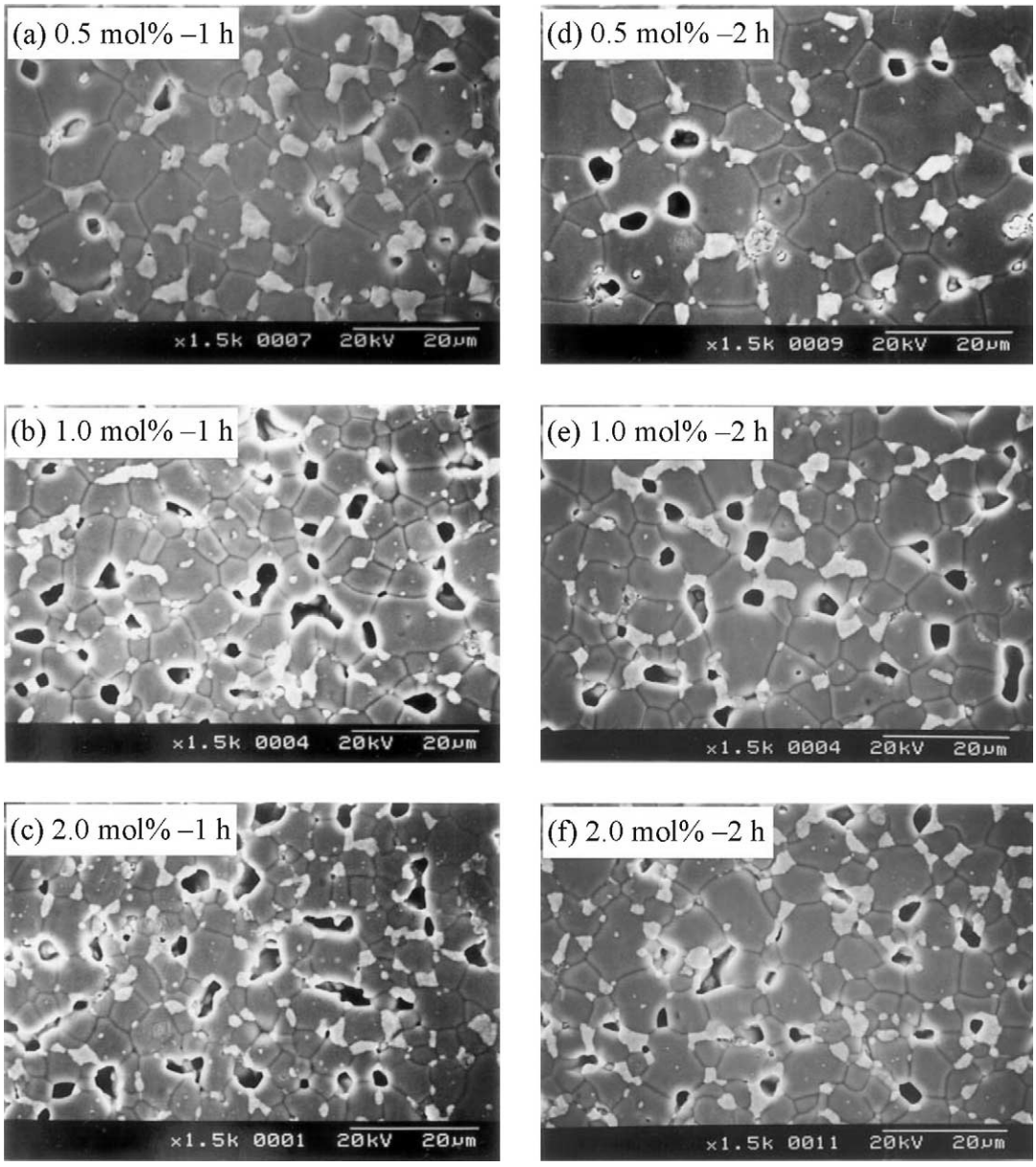

Fig. 1. SEM micrographs of ZPCCE ceramics sintered at 134 °C for 1–2 h with Er_2O_3 content.

Table 1
The microstructural parameters of ZPCCE ceramics sintered at 1340 °C for 1–2 h with Er_2O_3 content

Sintering time	Er_2O_3 content (mol%)	d (μm)	ρ (g/cm^3)	S (%)	P (%)
1 h	0.5	9.7	5.4	18.1	6.6
	1.0	7.0	4.9	15.5	15.2
	2.0	5.1	4.9	15.3	15.2
2 h	0.5	12.1	5.6	18.9	3.1
	1.0	8.5	5.2	17.2	10.0
	2.0	6.8	5.4	17.3	6.6

The density of ceramics was in the range of 5.4–4.9 g/cm^3 corresponding to 93.4–84.8% of theoretical density (TD = 5.78 g/cm^3) for sintering time of 1 h and 5.6–5.2 g/cm^3 corresponding to 96.9–90.0% of TD for 2 h. The density of ceramics exhibited a maximum at Er_2O_3 content of 0.5 mol% for both sintering times. The density greatly affects the resistance of degradation together with a leakage current in the V–I characteristics and a dielectric dissipation factor. This will be discussed in more detail later.

Fig. 2 shows the electric field–current density (E–J) characteristics of ZPCCE varistors sintered at 1340 °C for 1–2 h with Er_2O_3 content. All varistors are likely to exhibit good characteristics seemingly. The variation of V–I characteristic parameters, including the varistor voltage (V_{1mA}), varistor voltage per grain boundary (V_{gb}), nonlinear exponent (α), and leakage current (I_l) are summarized in Table 2. The $V_{1\ mA}$ increased in the range of 242.4–467.4 V/mm for sintering time of 1 h and 175.0–383.5 V/mm for 2 h with increasing Er_2O_3 content. As the $V_{1\ mA}$ is directly related to the number of grain boundaries across a series between the electrodes, the increase of $V_{1\ mA}$ with increasing Er_2O_3 content is attributed to the decrease of average grain size only. As the same meaning, a longer sintering time resulted in the decrease of $V_{1\ mA}$, due to the increase of average grain size. The V_{gb}, average breakdown voltage per grain boundaries, is defined as follows: $V_{gb} = (d/D) \cdot V_{1\ mA}$, where d is the average grain size and D is the thickness of sample. The V_{gb} was in the range of 2.4–2.5 V/gb for

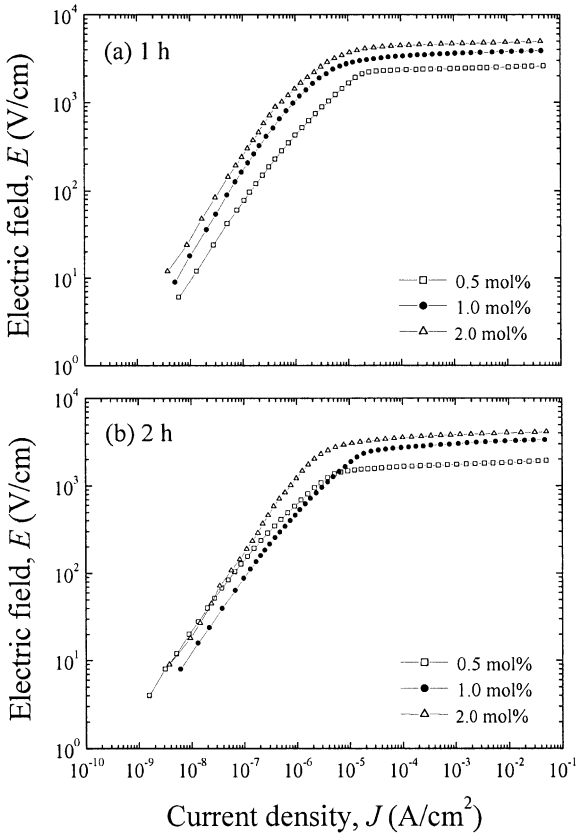

Fig. 2. The E–J characteristics of ZPCCE varistors sintered at 1340 °C for 1–2 h with Er_2O_3 content.

sintering time of 1 h and 2.1–2.6 V/gb for 2 h with Er_2O_3 content. This agrees to generally well-known 2–3 V/gb regardless of sintering processes and varistor compositions.

One of the most important figures of merits in varistors is the nonlinear exponent (α), which characterizes the native properties of varistor itself. Fig. 3 shows the nonlinear exponent (α) and leakage current (I_l) as a function of Er_2O_3 content of ZPCCE varistors sintered at 1340 °C for 1–2 h. The varistors sintered for 1 h exhibited a high value above $\alpha = 50$. In particular, the varistors with 0.5 and 2.0 mol% Er_2O_3 were found to be above $\alpha = 60$. The varistors sintered for 2 h also exhibited relatively high nonlinearity except for 1.0 mol%.

Table 2
The V–I and C–V characteristic parameters of ZPCCE varistors sintered at 1340 °C for 1–2 h with Er_2O_3 content

Sintering time	Er_2O_3 content (mol%)	V_{1mA} (V/mm)	V_{gb} (V/gb)	α	I_l (μA)	N_d (10^{18} cm^{-3})	N_t (10^{12} cm^{-2})	δ_b (eV)	t (nm)
1 h	0.5	242.4	2.4	61.2	2.8	1.14	3.60	1.211	31.58
	1.0	362.2	2.5	52.4	2.6	0.87	2.82	0.971	32.41
	2.0	467.4	2.4	61.4	2.3	1.26	4.00	1.345	31.75
2 h	0.5	175.0	2.1	43.4	1.2	1.48	3.79	1.034	25.61
	1.0	302.4	2.6	30.8	4.2	0.84	2.50	0.790	29.76
	2.0	383.5	2.6	51.4	2.2	0.97	2.48	0.680	25.57

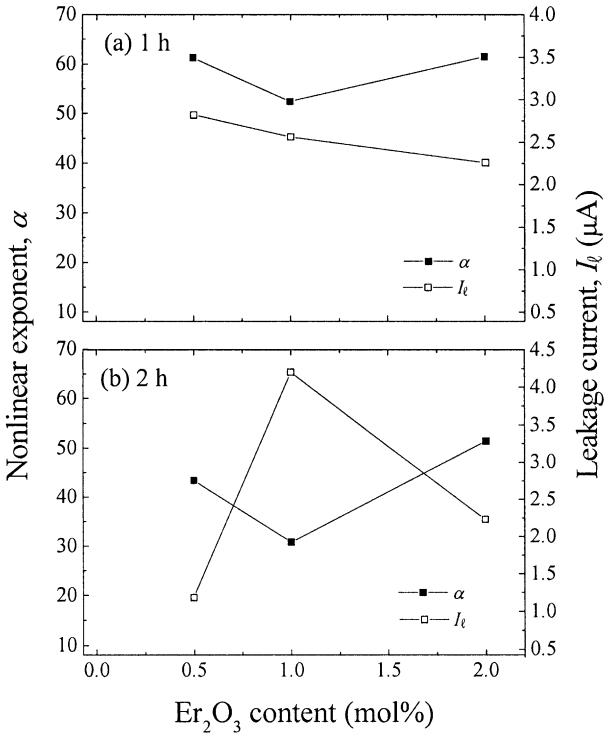

Fig. 3. The Nonlinear exponent and leakage current as a function of Er_2O_3 content of ZPCCE varistors sintered at 1340 °C for 1–2 h.

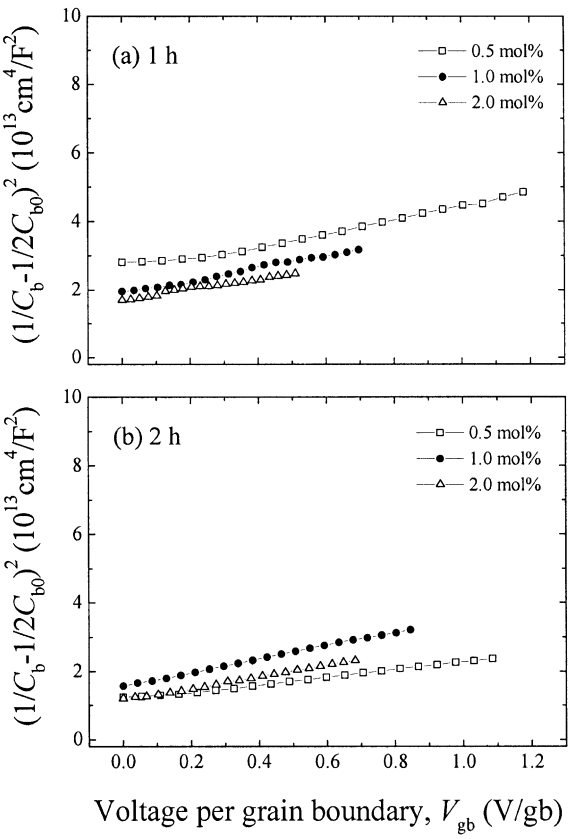

Fig. 4. The *C–V* characteristics of ZPCCE varistors sintered at 1340 °C for 1–2 h with Er_2O_3 content.

For both sintering times, the α value was decreased with increasing Er_2O_3 content. However, increasing additive content further to 2.0 mol% caused the α value to increase. The α value varied with a V-shape, reaching a minimum at 1.0 mol%. The maximum of α was obtained for the varistors with 2.0 mol% Er_2O_3, reaching $\alpha = 61.4$ for sintering time of 1 h and $\alpha = 51.4$ for 2 h. A longer sintering time decreased the α. In addition, it should be emphasized that the varistor with 0.5 mol% sintered for 1 h also exhibited high nonlinearity comparable to the varistors with 2.0 mol% sintered for 1 h. It was found that the addition of Cr_2O_3 to ZPCE ceramics greatly improves a nonlinearity of varistors [16]. However, the varistor with 1.0 mol% sintered for 2 h exhibited worse nonlinearity than that of ZPCE varistors. The I_l value of varistors sintered for 1 h was slightly decreased in the range of 2.8–2.3 μA with increasing Er_2O_3 content. As Er_2O_3 content is increased, the I_l value of varistors sintered for 2 h was increased, exhibiting a maximum (4.2 μA) for 1.0 mol% Er_2O_3. Increasing additive content further to 2.0 mol% caused the I_l value (2.2 μA) to decrease. The minimum of I_l was obtained for the varistors with 0.5 mol% Er_2O_3, reaching a minimum (1.2 μA). It is greatly expected that this varistors will reveal a high stability due to the highest density and the lowest leakage current.

Fig. 4 shows the *C–V* characteristics of ZPCCE varistors sintered at 1340 °C for 1–2 h with Er_2O_3 content. The *C–V* characteristic parameters, including the donor concentration (N_d), density of interface states (N_t), barrier height (ϕ_b), and depletion layer width (t) are summarized in Table 2. The values of N_d were in the range of 0.87×10^{18}–1.28×10^{18} cm^{-3} for sintering time of 1 h and in the range of 0.84×10^{18}–1.48×10^{18} cm^{-3} for 2 h, reaching a minimum at 1.0 mol% for both sintering time. With increasing Er_2O_3 content, the variations of N_t and ϕ_b also were similar to those of the N_d for sintering time of 1 h, whereas they were slightly decreased for 2 h. The t is related to theN_d and N_t, as indicated previously. In other words, the small N_d and large N_t lead to a large t. In gross, the values of *C–V* parameters for sintering time of 2 h exhibited to be decreased compared with those of 1 h.

In an application of varistors, ZnO varistors are always subjected to a continuous electrical stress. If the stability of varistors against stress is poor, the application of such varistors is extremely limited even if their nonlinearity is very superior. In practice, ZnO varistors begin to degrade because of gradually increasing leakage current with stress time. Eventually, they cause the thermal runaway and the loss of varistor function. The stability of the varistor is more important than any other properties. From this point of view, in addition to nonlinearity, the electrical stability is technologically very important characteristics of ZnO varistors. Fig. 5

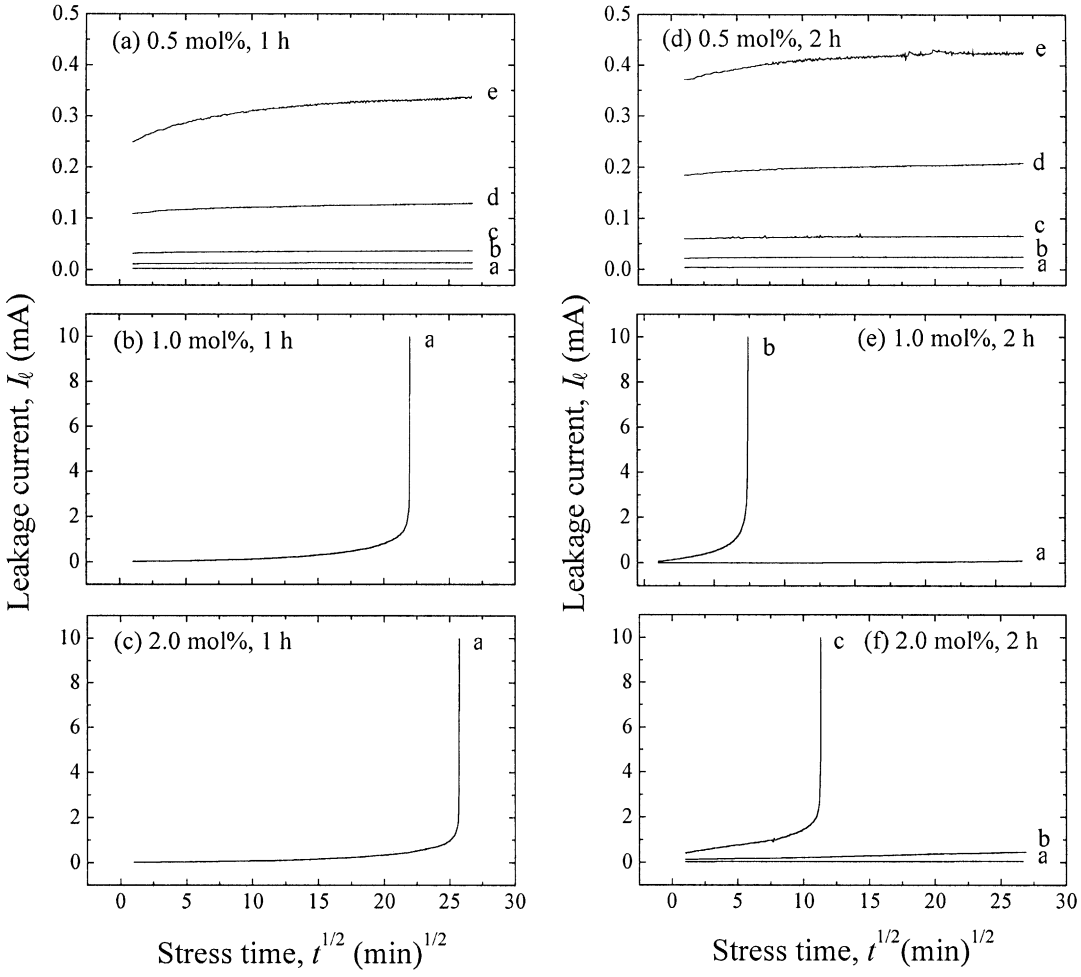

Fig. 5. The leakage current during various DC accelerated aging stresses of ZPCCE varistors sintered at 134 °C for 1–2 h with Er_2O_3 content. (a) the first stress, (b) the second stress, (c) the third stress, (d) the fourth stress, and (e) the fifth stress.

shows the leakage current during various DC accelerated aging stresses of ZPCCE varistors sintered at 1340 °C for 1–2 h with Er_2O_3 content. ZPCCE varistors with 1.0 and 2.0 mol% Er_2O_3 sintered for 1 h, even under relatively weak stress, exhibited the thermal runaway within a short time. This poor stability may be attributed to essentially low ceramic density, which decreases the number of parallel conduction path and eventually leads to the concentration of current. In these varistors, the leakage current is low, but the ceramic density is very low. It is suggested that the stability is more predominantly affected by the density than the leakage current. The thermal runaway of the varistor with 1.0 mol% Er_2O_3 sintered for 2 h can be analyzed in the same meaning above. By the way, although the varistor with 2.0 mol% Er_2O_3 sintered for 2 h possesses similar ceramic density and leakage current compared with the varistor with 0.5 mol% Er_2O_3 sintered for 1 h, this exhibited the thermal runaway at the third stress. It is supposed that this phenomenon is related to the dielectric dissipation factor (tanδ). Really, all varistors having relatively high tanδ caused the thermal runaway as (b), (c), (e), and (f) in Fig. 5. The tanδ of ZPCCE varistors measured at 1 kHz and 1 V_{rms} are summarized in Table 3. The tanδ of varistor with 2.0 mol% Er_2O_3 sintered for 2 h was 12.7%, which is much higher than the tanδ (3.8%) of varistor 0.5 mol% Er_2O_3 sintered for 1 h. In these viewpoints, the stability of varistors seems to be affected by tan δ, in addition to the ceramic density and leakage current.

On the other hand, the varistors with 0.5 mol% Er_2O_3 exhibited much higher stability, compared with the varistors with 1.0 and 2.0 mol% Er_2O_3. It can be seen that their leakage current is nearly constant until the fourth stress and shows weak positive creep during the fifth stress. The stability of varistors can be explained by degradation rate coefficient (K_T), indicated by the expression $I_l = I_{lo} + K_T\ t^{1/2}$.[19] For the varistors doped with 0.5 mol% Er_2O_3, the K_T for 1 h is lower than that for 2 h until the fourth stress, whereas the K_T in the fifth stress was +16.18 μA $h^{-1/2}$ for sintering time of 1 h and +11.23 μA $h^{-1/2}$ for 2 h. Therefore, the varistors sintered for 2 h are electrically more stable than those for 1 h.

Fig. 6 shows the variation of *V–I* characteristic parameters, such as variation rate of the varistor voltage ($\%\Delta V_{1\ mA}$), variation rate of the nonlinear exponent ($\%\Delta\alpha$), and variation rate of the leakage current ($\%\Delta I_l$) after various DC accelerated aging stresses, for the varistors sintered at 1340 °C for 1–2 h with 0.5 mol% Er_2O_3, with no thermal runaway even under the fifth stress. In an aspect of the stability of *V–I* characteristics, the $\%\Delta V_{1\ mA}$ should be lower than any other variation rate of parameters. In general, the allowed specifications of $\%\Delta V_{1\ mA}$ for the commercial varistors are less than 10% under 0.85 $V_{1\ mA}$/85 °C/1000 h. Even though the stressing time in this study is

Table 3
The dielectric dissipation factor (tanδ) of ZPCCE varistors sintered at 1340 °C for 1–2 h with Er_2O_3 content

Sintering time	Er_2O_3 content (mol%)	tan δ (%)
1 h	0.5	3.8
	1.0	8.9
	2.0	14.2
2 h	0.5	4.8
	1.0	11.4
	2.0	12.7

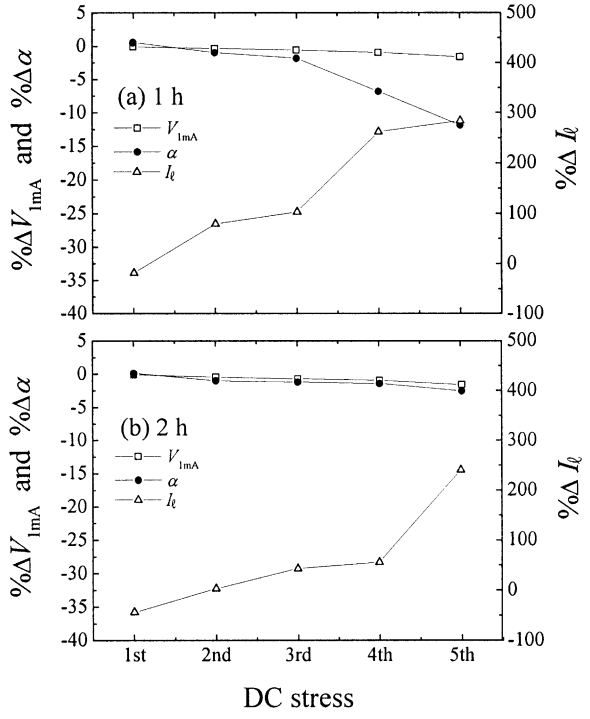

Fig. 6. The variation rate of *V–I* characteristic parameters as a function of DC accelerated aging stress of ZPCCE varistors sintered at 1340 °C for 1–2 h with 0.5 mol% Er_2O_3.

Table 4
The variation of *V–I* characteristic parameters after various DC accelerated aging stresses of ZPCCE varistors sintered at 1340 °C for 1–2 h with Er_2O_3 content

Sintering time	Er_2O_3 content (mol%)	Stress condition	K_T ($\mu A\ h^{-1/2}$)	$V_{1\ mA}$ (V/mm)	$\%\Delta V_{1\ mA}$	α	%Δα	I_l (μA)	$\%\Delta I_l$
1 h	0.5	Before		242.4	0	61.2	0	2.8	0
		First	0.02	242.4	0	61.6	0.6	2.3	−17.9
		Second	0.3	241.7	−0.30	60.7	−0.8	5.1	82.1
		Third	0.9	241.1	−0.54	60.2	−1.6	5.7	103.6
		Fourth	4.1	240.2	−0.91	57.1	−6.7	10.2	264.3
		Fifth	16.2	238.7	−1.53	54.0	−11.8	10.8	285.7
	1.0	Before		362.2	0	52.4	0	2.6	0
		First			Thermal runaway				
	2.0	Before		467.4	0	61.4	0	2.3	0
		First			Thermal runaway				
2 h	0.5	Before		175.0	0	43.4	0	1.2	0
		First	0.1	174.9	−0.06	43.4	0	0.7	−41.7
		Second	0.5	174.3	−0.40	42.9	−1.2	1.2	0
		Third	1.0	173.8	−0.69	42.9	−1.2	1.7	41.7
		Fourth	5.0	173.3	−0.97	42.8	−1.4	1.8	50.0
		Fifth	11.2	172.3	−1.54	42.3	−2.5	4.0	233.3
	1.0	Before		302.4	0	30.8	0	4.2	0
		First	30.1	297.2	−1.72	26.5	−14.0	4.8	14.3
		Second			Thermal runaway				
	2.0	Before		383.5	0	51.4	0	2.2	0
		First	5.3	382.0	−.0.39	48.6	−5.5	3.1	40.9
		Second	111.3	373.8	−2.53	39.9	−22.4	6.5	195.5
		Third			Thermal runaway				

short, the stressing voltage and ambient temperature are very severe. Therefore, it is believed that these DC accelerated aging stresses are very severe. As mentioned in *V–I* characteristics previously, the varistors with 0.5 mol% Er_2O_3 sintered for 1 h have exhibited very high nonlinearity. These varistors, for DC accelerated aging stress, exhibited a high stability by marking $\%\Delta V_{1\ mA} = -1.5\%, \%\Delta\alpha = -11.8\%$, and $\%\Delta I_{l=} + 285.7\%$ after the fifth stress. It is forecasted that these varistors will be sufficiently applied to surge absorbers.

While, even though the varistors with 0.5 mol% Er_2O_3 sintered for 2 h are relatively low compared with those for 1 h, they also have a high nonlinearity. Furthermore, they exhibited excellent stability, in which $\%\Delta V_{1\ mA} = -1.5\%$, $\%\Delta\alpha = -2.5\%$, and $\%\Delta I_l = +233.3\%$ after the fifth stress. These values were the lowest variation rates in Pr_6O_{11}-based ZnO varistors, which have been studied so far. This high stability may be attributed to the high density (5.6 g/cm^3), and the low leakage current (1.2 μA), the low tan δ (4.8) ultimately. As a result, the varistors with 0.5 mol% Er_2O_3 sintered for 2 h exhibited the best performance in terms of the densification, nonlinearity, and stability. Therefore, it is believed that the varistors with 0.5 mol% Er_2O_3 sintered for 2 h will be diversely applied to surge protection systems. The detailed *V–I* characteristic parameters of ZPCCE varistors after various DC accelerated aging stresses are summarized in Table 4.

Table 4 The variation of *V–I* characteristic parameters after various DC accelerated aging stresses of ZPCCE varistors sintered at 1340 °C for 1–2 h with Er_2O_3 content.

4. Conclusions

The microstructure, voltage–current (*V–I*) characteristics, capacitance–voltage (*C–V*) characteristics, and *V–I* stability of ZPCCE ($ZnO–Pr_6O_{11}–CoO–Cr_2O_3–Er_2O_3$) based varistors were investigated with Er_2O_3 content and sintering time. The varistors with 2.0 mol% Er_2O_3 sintered for 1 h exhibited an excellent nonlinearity, with a nonlinear exponent of 61.4 and a leakage current of 2.3 μA. However, they exhibited very low stability, due to the low ceramic density and high dielectric dissipation factor (tan δ). On the other hand, the varistors with 0.5 mol% Er_2O_3 exhibited a high nonlinearity and stability. In particular, the varistors sintered for 2 h exhibited not only a relatively high nonlinear exponent of 43.4 and low leakage current of 1.2 μA, but also the highest electrical stability, in which $\%\Delta V_{1\ mA}$ = -1.5%, $\%\Delta\alpha = -2.5\%$, and $\%\Delta I_{l=} + 233.3\%$ in the *V–I* characteristics, under DC accelerated aging stress, such as $(0.80V_{1\ mA}/90\ °C/12\ h) + (0.85V_{1\ mA}/115\ °C/12\ h) + (0.90V_{1\ mA}/120\ °C/12\ h) + (0.95V_{1\ mA}/125\ °C/12\ h) + (0.95V_{1\ mA}/150\ °C/12\ h)$. This is because they possessed high ceramic density, low leakage current, and low dissipation factor.

In conclusion, it was estimated that 97.5 mol% ZnO–0.5 mol% Pr_6O_{11}–1.0 mol% CoO–0.5 mol% Cr_2O_3–0.5 mol% Er_2O_3 based ceramics sintered for 2 h will be usefully applied to Pr_6O_{11}-based ZnO varistors for surge absorbers and arresters having the high performance and high stability in the future.

Acknowledgements

This article was financially supported by the Research Center for Electronic Ceramics (RCEC) of Dongeui University founded by the Korea Science and Engineering Foundation (KOSEF), Ministry of Science and Technology (MOST) and the Busan Metropolitan City Government.

References

1. Levinson, L. M. and Pilipp, H. R., Zinc oxide varistor—a review. *Am. Ceram. Soc. Bull.*, 1986, **65**, 639–646.
2. Gupta, T. K., Application of zinc oxide varistor. *J. Am. Ceram. Soc.*, 1990, **73**, 1817–1840.
3. Lee, Y. S. and Tseng, T. Y., Phase identification and electrical properties in ZnO-glass varistors. *J. Am. Ceram. Soc.*, 1992, **75**, 1636–1640.
4. Alles, A. B. and Burdick, V. L., The effect of liquid-phase sintering on the properties of Pr_6O_{11}-based ZnO varistors. *J. Appl. Phys*, 1991, **70**, 6883–6890.
5. Alles, A. B., Puskas, R., Callahan, G. and Burdick, V. L., Compositional effect on the liquid-phasse sintering of praseodymium oxides-based ZnO varistors. *J. Am. Ceram. Soc.*, 1993, **76**, 2098–2102.
6. Lee, Y. S., Liao, K. S. and Tseng, T. Y., Microstructure and crystal phases of praseodymium in zinc oxides varistor ceramics. *J. Am. Ceram. Soc.*, 1996, **79**, 2379–2384.
7. Wakiya, N., Chun, S. Y., Lee, C. H., Sakurai, O., Shinozaki, K. and Mizutani, N., Effect of liquid phase and vaporization on the formation of microstructure of Pr doped ZnO varistor. *J. Electroceram., 4:S1, 1999, 15–23.*
8. Chun, S. Y. and Mizutani, N., Mass transport via grain boundary in Pr-based ZnO varistors and related electrical effects. *Mater. Sci. Eng., B79, 2001, 1–5.*
9. Nahm, C. W. and Park, C. H., Microstucture, electrical properties, and degradation behavior of praseodymium oxides-based zinc oxide varistors doped with Y_2O_3. *J. Mat. Sci.*, 2000, **35**, 3037–3042.
10. Nahm, C. W., Park, C. H. and Yoon, H. S., Highly stable nonohmic characteristics of $ZnO–Pr_6O_{11}–CoO–Dy_2O_3$ based varistors. *J. Mat. Sci. Lett.*, 2000, **19**, 725–728.
11. Nahm, C. W., The electrical properties and d. *c. degradation characteristics of Dy_2O_3 doped Pr_6O_{11}-based ZnO varistors. J. Eur. Ceram. Soc.*, 2001, **21**, 545–553.
12. Nahm, C. W. and Park, C. H., Effect of Er_2O_3 addition on the microstructure, electrical properties, and stability of Pr_6O_{11}-based ZnO ceramic varistors. *J. Mat. Sci.*, 2001, **36**, 1671–1677.

13. Nahm, C. W., The nonlinear properties and stability of ZnO–Pr_6O_{11}–CoO–Cr_2O_3–Er_2O_3 ceramic varistors. *Mater. Lett*., 2001, **47**, 182–187.
14. Nahm, C. W., Yoon, H. S. and Ryu, J. S., The nonlinear properties and d. c. degradation characteristics of ZPCCE based varistors. *J. Mater. Sci. Lett*., 2001, **20**, 393–395.
15. Nahm, C. W. and Ryu, J. S., Influence of sintering temperature on varistor characteristics of ZPCCE-based ceramics. *Mater. Lett*., 2002, **53**, 110–116.
16. Mukae, M., Tsuda, K. and Nagasawa, I., Capacitance-vs-voltage characteristics of ZnO varistor. *J. Appl. Phys*, 1979, **50**, 4475–4476.
17. Hozer, L., *Semiconductor Ceramics: Grain Boundary Effects*, Ellis Horwood, 1994.
18. Wurst, J. C. and Nelson, J. A., Lineal intercept technique for measuring grain size in two-phase polycrystalline ceramics. *J. Am. Ceram. Soc*., 1972, **55**, 109–111.
19. Fan, J. and Freer, R., Deep level transient spectroscopy of zinc oxide varistors doped with aluminum oxide and/or silver oxide. *J. Am. Ceram. Soc*., 1994, **77**, 2663–2668.